CERN-ACC-Note-2018-0021

March 2018

Report from LHC MD 2158: IR-nonlinear studies

E.H. Maclean, F. Carlier, J.W. Dilly, M.S Camillocci, E. Cruz Alaniz, B. Dalena, E. Fol, K. Fuchsberger, M. Giovannozzi, M. Hofer, L. Malina T.H.B. Persson, J. Coello de Portugal, P. Skowronski, R. Tomás, A. Garcia-Tabares Valdivieso, A. Wegscheider

Keywords: LHC, nonlinear errors, experimental insertions

Summary

For the first time the LHC is running for luminosity-production with local corrections for nonlinear errors in the ATLAS and CMS insertions. While a major step forward in LHC optics commissioning strategy (and one which has yielded clear operational benefits) considerable challenges remain to be overcome, both in regard to the optimization of LHC optics and in order to ensure successful commissioning of the High-Luminosity LHC. MD 2158 sought to follow up several aspects of the 2017 nonlinear optics commissioning which are not yet understood, and by enhancing sextupole and dodecapole sources in the ATLAS and CMS insertions explore the prospects for linear and nonlinear optics commissioning in the HL-LHC.

Contents

1 Motivation and description

Beam commissioning in 2017 saw, for the first time, corrections of nonlinear errors in low-β insertions implemented operationally in the LHC. Normal/skew sextupole and normal/skew octupole errors were compensated in IR1, while normal sextupoles and octupoles were compensated in IR5. The benefits of this beam-based nonlinear compensation to LHC operation were clear, specifically: improved stability of linear optics, improved control of linear coupling, improved performance of beam-instrumentation, reduced variability of the tune footprint throughout the LHC cycle, and reduced strength of key sextupole and octupole resonances [1, 2].

While extremely successful, 2017 commissioning left open a number of questions. No corrections for skew errors were applied in IR5. In the case of a_4 (skew octupole) this was justified by studies in 2016, which showed a significantly smaller quadratic variation of linear coupling as a function of crossing-angle than was present in IR1 [3]. In the case of a_3 (skew sextupole), the observed feed-down to linear coupling during commissioning was also comparatively small. With limited time available for measurement and correction of these errors, priority was therefore given to a large feed-down to $|C^-|$ observed in IR1. None-the-less, compensation of a_3 remains of particular interest for both the LHC and HL-LHC, due to its role in driving the $3Q_y$ resonance, while footprint distortion and amplitude-dependent closest-tune approach driven by skew octupoles is also gaining traction as a potential limit on HL-LHC operability [1, 4, 5]. For the MD2 session in 2017 it was desired to follow-up study of skew sextupoles by examining feed-down from a crossing-angle bump in the vertical plane of IR5. The nominal crossing angle in IR5 lies in the horizontal plane, resulting in a feed-down from skew sextupole errors to linear coupling. By scanning crossing-angle in the vertical plane the a_3 errors instead feed-down to tune. This represents a more straightforward measurement than feed-down to coupling, and in IR1 (where the nominal crossing angle is vertical) minimization of tune feed-down during commissioning was seen to reduce $|f'_{0030}|$, an AC-dipole resonance driving term (RDT) [6] related to the strength of the $3Q_y$ resonance .

During 2017 commissioning, corrections for normal octupole (b_4) errors were applied in IR1 and IR5. This correction had been tested in previous years, and seen to substantially reduce the strength of the $4Q_x$ resonance [3] and improve lifetime at $\beta^* = 0.14\,\mathrm{m}$ [3]. Upon application at the start of the commissioning block, the b_4 correction was observed to improve the performance of tune and coupling measurement by the LHC BBQ [7, 8]. Measurements at $\beta^* = 0.3\,\mathrm{m}$, with a flat-orbit, explicitly demonstrated an excellent correction of the amplitude detuning. At the end of the commissioning block however, when measurements were performed at $0.4\,\mathrm{m}$ with the nominal crossing scheme applied in all IPs, a substantial amplitude detuning was measured [7, 8]. The tune shift was non-negligible, corresponding to the equivalent of $\sim \pm 90\,\mathrm{A}$ of Landau octupole powering (dependent on the beam and plane in question). BBQ data indicated a drift of the unperturbed tune during the measurement, which offers a potential explanation, however BBQ data during the anomalous measurement was also of poor quality (with noise comparable to the shift in question). Another possible explanation for the extra detuning, was as the result of feed-down to b_4 from an even higher-order error. Measurements of IR5 in 2016 showed no notable change to amplitude detuning when the IP5 crossing angle was applied [3]. IP1, however, had never been studied and remained a potential source. It was planned to measure amplitude detuning at crossing angles of $\pm 150\,\mu\mathrm{rad}$ in IR1, with a flat-orbit elsewhere in the machine. This would confirm whether IR1 was the source of the anomalous detuning observed during commissioning, and allow an identification of the multipole order of any source.

While further optimization of LHC nonlinear optics is a priority, prospects for linear and non-

linear commissioning of the HL-LHC also need to be addressed. Operating at lower β^* and larger crossing-angles, the impact of nonlinear errors on both linear and nonlinear optics is expected to increase significantly. This may be detrimental to commissioning efforts, with increased nonlinearity of the accelerator leading to deterioration in beam-quality; but also advantageous, with new observables becoming viable. It is not possible to directly replicate the conditions of HL-LHC commissioning at small β^* during LHC MDs. By using the nonlinear correctors in the IPs to enhance the nonlinear sources however, it is possible to make a crude approximation of conditions which may be present in the HL-LHC. For this MD the skew sextupole corrector on the right side of IP1 was powered to $100\,\mathrm{A}$, compared to its $\sim 20\,\mathrm{A}$ setting obtained via beam-based correction. This scaling is both representative of the $3Q_y$ strength (scaling as $\sim (1/\beta^*)^{\frac{3}{2}}$) at $0.15\,\mathrm{m}$ which may be expected in the HL-LHC, and of the feed-down to linear optics perturbations (which scale as $1/\beta^*$ and linearly with the expected increase in crossing angle for the HL-LHC). In this configuration linear optics measurements were performed at flat-orbit, and with $\pm 150\,\mu\mathrm{rad}$ crossing-angle in IR1. This enables a first study into how strong skew sextupole sources may impact linear optics measurement in the HL-LHC. Beyond this initial motivation, it is also of interest to study whether the segment-by-segment technique (normally used for local linear optics correction in the LHC) [9, 10] can be applied to sextupolar feed-down in the HL-LHC. Finally, the enhancement of the sextupole resonances should provide an indication of the likely measurement quality which can be obtained in the HL-LHC.

In the HL-LHC even decapole and dodecapole compensation is expected to be essential for successful operation. With the IR-a_3 correctors returned to their operational values, the b_6 correctors in IP1 and IP5 were ramped up to their maximum available current, in order to reproduce the second-order amplitude detuning expected in the HL-LHC. Large amplitude kicks were performed at flat-orbit to check the possibility to measure dodecapolar RDTs and second-order detuning. A crossing angle was then applied in IP1 to check the viability for measurement of feed-down from b_6 to b_4 as a potential observable for dodecapole correction in the HL-LHC.

2 Measurement Summary

Table 1 summarizes key parameters of the MD. A detailed timeline of the MD is given in Tab. 2. As many of the measurements performed during this MD involved comparisons between nonlinear observables measured in different machine states, it was necessary to ensure coupling was well controlled throughout the MD [11] (otherwise it may be unclear whether shifts in a given parameter relate directly to the change of machine state or are induced by shifts to coupling). Consequently AC-dipole based coupling corrections were applied following every significant change in machine state. Injection tunes were utilized throughout the MD in order to prevent the linear coupling stop-band interfering with feed-down measurements, and move the working point further from the $3Q_y$ resonance. This procedure was the same as that employed throughout Run 2 commissioning. Finally corrections for orbit leakage were implemented following any change in crossing angle.

Table 1: Measurement summary.

Objective:	Various studies of nonlinearities in the low-β insertions
MD #:	2158
FILL #:	5995
Beam Process:	MD → SQUEEZE-6.5TeV-1m-40cm-2017_V1_MD2@467[END]
Date:	25/07/2017
Start Time:	07:30
End Time:	15:30

3 Results

Results from measurements indicated in **bold** in Tab. 2 are discussed in the following sections.

3.1 Vertical crossing angle scan in IP5

The horizontal orientation of the crossing angle in IR5 results in skew sextupole errors (a_3) feeding-down to linear coupling. By contrast a vertical offset causes feed-down to normal quadrupole, resulting in a tune shift. In simulation, using skew sextupole correctors in IR5 to compensate the linear tune shift with vertical crossing angle, also elicited a compensation of feed-down to linear coupling with horizontal crossing angle. This is illustrated in Fig. 1 which shows a simulation of feed-down from the a_3 errors of WISE seed 1 for vertical (left) and horizontal (right) crossing angles in IR5. Only a_3 sources were applied. Errors were only applied in the IR. Red data indicates the uncompensated feed-down. Blue data shows the feed-down obtained when the MCSSX3.[LR5] were powered in simulation to compensate the linear variation of tune with vertical crossing angle. These same settings were applied to simulations of the horizontal crossing scan (right plots, blue data) resulting in a correction of the feed-down to coupling. Measurement of tune vs crossing angle is more straightforward than the coupling study, which requires AC-dipole excitation. Simultaneous compensation of feed-down in both crossing planes also provides a more robust test of the nonlinear corrections than is possible with a single variable, helping ensure local compensation of errors within the IRs and making feed-down studies in the non-conventional planes a potentially useful tool for study of the nonlinearities.

Table 2: Timeline of the MD. Key measurements are indicated in **bold**.

07:00:00	Scheduled start of MD
07:30:00	First injection for MD (previous MD over-ran)
07:30:00→07:45:00	ϵ_{B2H} too large. Re-steering performed
07:45:00	Injection of bunches for MD
08:00:00	Start of ramp
08:35:00	Arrive at $40\,\mathrm{cm}$
08:40:00→09:18:00	Retracting collimators
09:20:00→09:55:00	Move to flat-orbit. Orbit correction
09:55:00	Move to injection tunes $(0.28, 0.31)$
09:58:00→10:03:00	Chromaticity corrected to $3\,\mathrm{units}$. Tune correction.
10:05:00→10:19:00	Coupling correction via AC-dipole. $\lvert C^- \rvert < 1 \times 10^{-3}$
10:19:00→10:34:00	Take flat reference orbit for rest of MD
10:36:00→10:54:30	**IP5-V crossing angle scan**
10:56:00	IP1-V crossing angle to $+150\,\mu\mathrm{rad}$. Leakage correction.
10:58:00	Tune correction
11:02:00	Coupling correction via AC-dipole
11:06:00→11:30:00	**Amplitude detuning with IP1V crossing angle**
11:11:00→11:15:00	Detuning measurement interrupted. (*Jorg/Lukas apply orbit bump to check something with BPMs*)
11:30:00	IP1-V crossing angle to $-150\,\mu\mathrm{rad}$. Q-FB on. Leakage correction.
11:38:00	B1 coupling correction via AC-dipole
11:39:00	B2 coupling correction via AC-dipole
11:43:00	B2 coupling correction via AC-dipole (2^{nd} iteration)
11:40:00→11:55:00	**Beam 1: amplitude detuning with $-$IP1V crossing angle**
11:43:30→12:04:00	**Beam 2: amplitude detuning with $-$IP1V crossing angle**
12:05:00	Back to flat-orbit. Leakage correction.
12:06:15	Tune correction
12:12:12	B1 coupling correction via AC-dipole (no B2 correction needed)
12:12:30	**AC-dipole measurement for RDT baseline**
12:22:00→12:31:00	**MCSSX trimmed to $+100\,\mathrm{A}$. Q-FB on.**
12:31:30→12:37:00	Coupling correction via AC-dipole
12:37:00→12:53:30	**Linear optics measurement via AC-dipole. Flat-orbit. Strong MCSSX.**
12:54:00	IP1-V crossing angle to $+150\,\mu\mathrm{rad}$. Leakage correction.
12:55:30	Tune correction. **No coupling correction.**
12:57:00→13:18:30	**Linear optics via AC-dipole. IP1V crossing angle. Strong MCSSX.**
13:20:30	IP1-V to $-150\,\mu\mathrm{rad}$. Q-FB on. Leakage correction. **No $\lvert C^- \rvert$ corr**
13:24:00→13:40:00	**Linear optics via AC-dipole. $-$IP1V crossing angle. Strong MCSSX.**
13:41:30	Return to flat-orbit. Q-FB on. Leakage correction.
13:43:00→13:50:00	**MCSSX trimmed to nominal setting. Q-FB on.**
13:51:00→13:55:00	**IP1/5 MCTX trimmed to $+50\,\mathrm{A}$. Q-FB on.**
13:55:00→14:07:00	AC-dipole coupling correction
14:07:00→14:45:00	**2^{nd}-order detuning measurement. Flat-orbit. Strong MCTX.**
14:45:00→14:53:00	**Diagonal kicks for RDT. Flat-orbit. Strong MCTX.**
14:54:00	IP1V crossing angle to $+150\,\mu\mathrm{rad}$. Q-FB on. Leakage correction.
14:55:00→15:03:00	Attempt detuning measurement. Losses too high.
15:04:00	IP1V crossing angle to $+75\,\mu\mathrm{rad}$. Q-FB on. Leakage correction.
15:05:00→15:21:00	**Amplitude detuning. $0.5\times$IP1V crossing angle. Strong MCTX.**
15:21:00→15:26:00	Return to flat-orbit. MCTX to $0\,\mathrm{A}$
15:27:00	MD ends

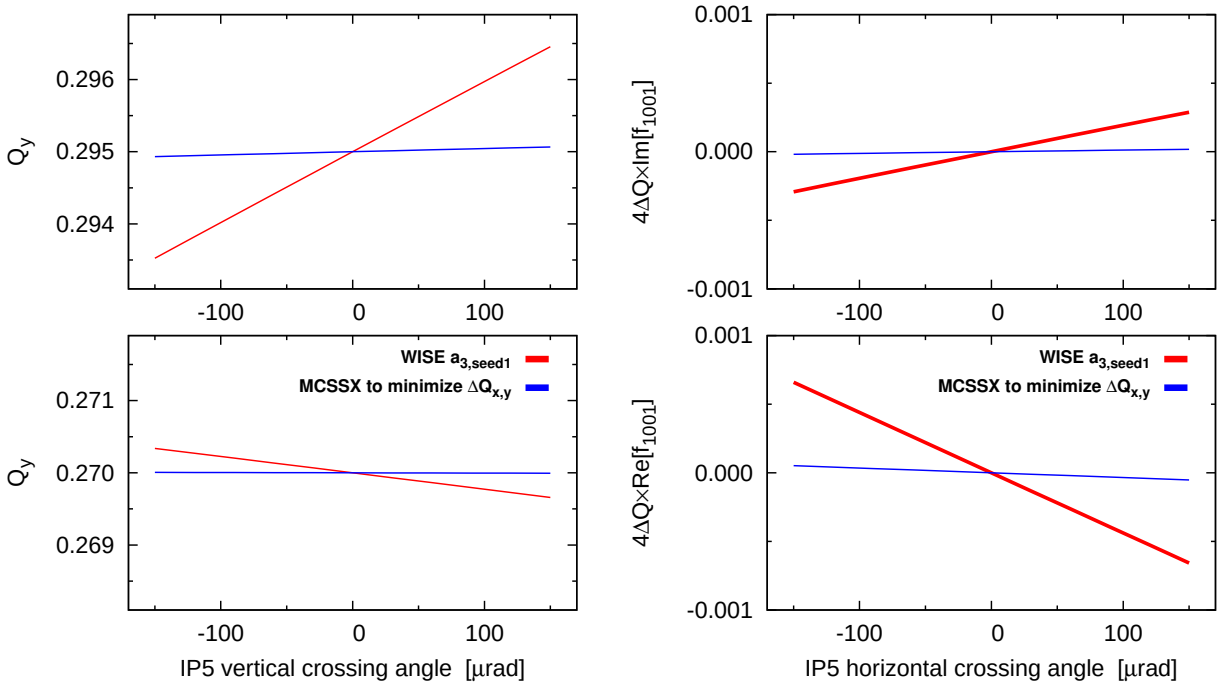

Figure 1: Simulation of feed-down to tune with vertical IP5 crossing angle (left), and feed-down to coupling with horizontal crossing angle (right), for skew sextupole errors of WISE seed 1 applied to $\mathrm{Q}_{1,2,3}$ and D_1. Red data indicates the feed-down from uncompensated errors. Blue simulations show feed-down for both cases when MCSSX.3[LR]5 are applied to minimize the linear variation of tune with vertical crossing angle.

Figure 2 shows the tune shifts measured for Beam 1 (left) and Beam 2 (right) during a scan of the vertical crossing angle. Measurements were performed to $\pm 150\,\mu\mathrm{rad}$ without difficulty, allowing sufficient range to examine the skew sextupole feed-down. Note that this study is concerned with the linear component of the tune variation. The quadratic part is generated via normal octupole (b_4) feed-down, and occurs for horizontal and vertical crossing angles. To try and determine corrections for skew sextupole errors, settings of the MCSSX in IR5 were sought to reproduce the linear variation of tune. Application of these settings in reverse should compensate the a_3 feed-down in the real machine. Since the errors and correctors are located in the common region of the IR corrections cannot be considered independently for the two beams.

Blue lines in Fig. 2 show the best match obtained to the linear variation of tune. It was not possible to find a single pair of settings for the MCSSX3.L5 and MCSSX3.R5 which simultaneously minimized the tunes of Beam 1 and Beam 2. In particular it is seen that the proposed correction does not compensate the linear variation of Q_x for Beam 2. It was not possible to improve this term without also significantly deteriorating the compensation of the other terms. This can also be observed in study of horizontal feed-down to coupling. Figure 3 shows the feed-down to linear coupling measured for a horizontal crossing angle scan of IP5 during 2017 commissioning. While corrector settings obtained from the vertical scan do a good job of matching the linear variation of the Beam 1 coupling, the effect on Beam 2 would be to deteriorate feed-down.

The discrepancies between Beam 1 and Beam 2, and between tune and coupling, are highly suggestive of feed-down from even higher-order errors (for example due to alignment or orbit effects). While the vertical crossing angle scan performed in this MD is of limited use to plan a_3 corrections in 2018 therefore, it establishes the need for accurate a_4 and b_4 corrections to be applied in IR5 before

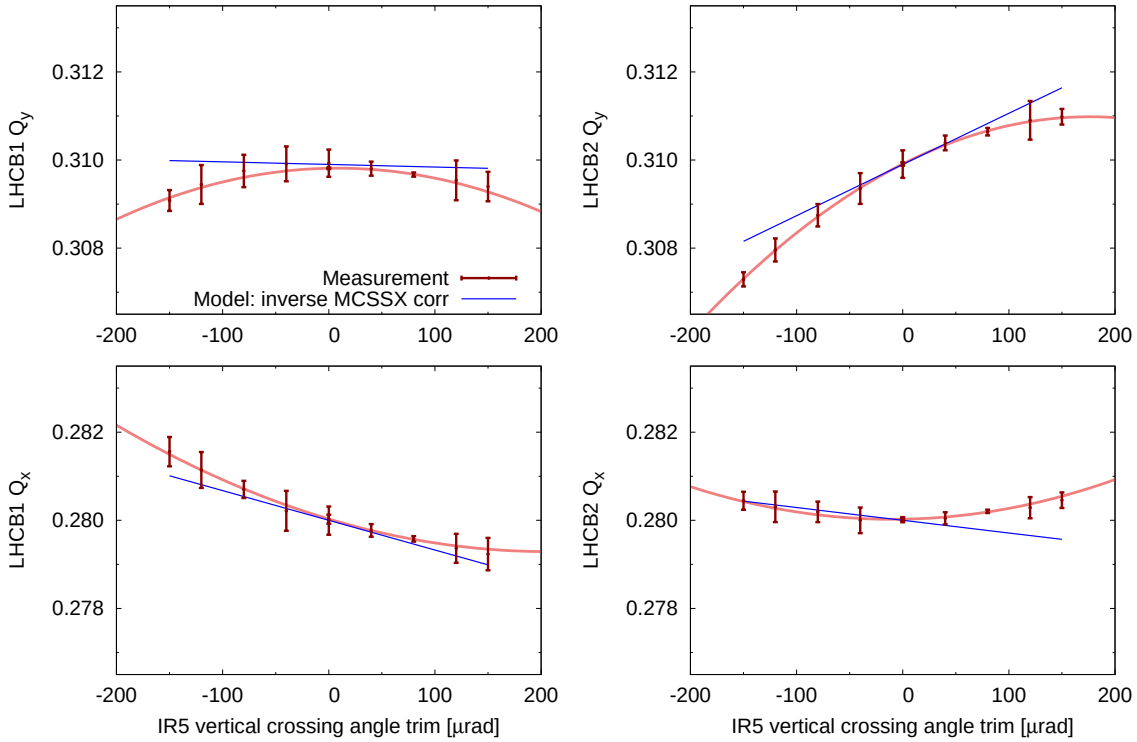

Figure 2: Feed-down to tune measured during a scan of the vertical crossing angle orbit bump through IR5. Note that the operational crossing angle for IR5 is oriented horizontally.

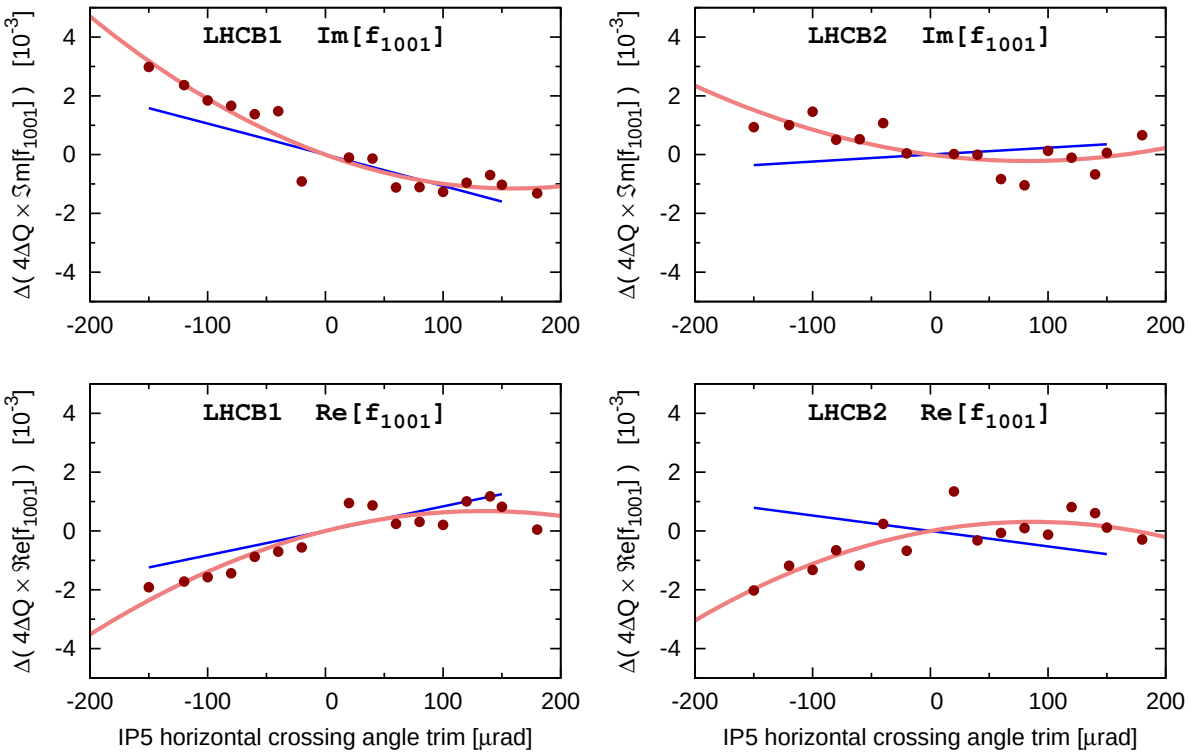

Figure 3: Feed-down to linear coupling measured during a scan of the IR5 horizontal crossing angle, during $\beta^* = 0.4\,\mathrm{cm}$ commissioning in 2017.

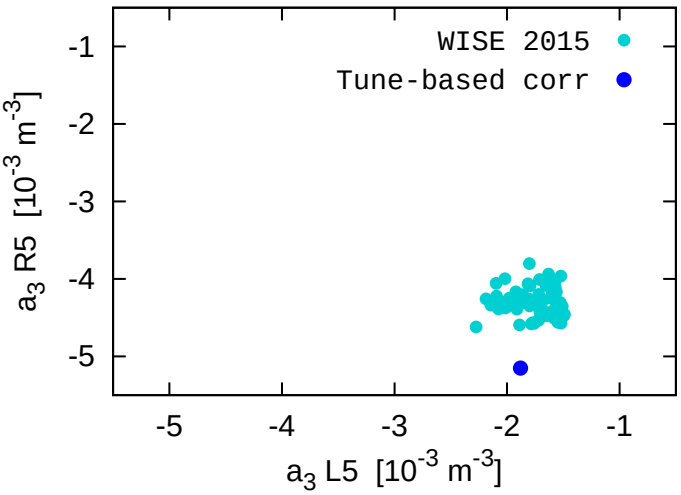

Figure 4: Nominal correction calculated from old and new versions of the WISE tables, compared to MCSSX settings based upon minimization of linear tune shift during a vertical crossing angle scan in IR5.

considering sextupole compensation. It is interesting to note that the best correction obtained from linear variation of tune with crossing-angle agrees well with that implied via the magnetic measurements, to which no reference was made during determination of the beam-based correction. While neither the beam-based nor magnetic corrections would fully compensate the observed feed-down from a_3, it appears to suggest that the magnetic model is not far removed from the true sources in the machine.

As regards a_3 correction, there are clearly issues between the two beams. 2018 commissioning therefore will require good initial corrections of the octupole errors in order to minimize additional sources coming from higher-order feed-down. Improved coupling measurement will be important, since the observations in Fig. 3 show large variation between AC-dipole kicks, creating larger uncertainties in any a_4 and a_3 corrections. Higher quality coupling measurements may be obtained, at the cost of additional commissioning time, via a dedicated scan with reduced tune separation. Finally it will be essential to validate a_3 compensation of both beams via RDTs.

3.2 Effect of IP1 crossing angle on amplitude detuning

While amplitude detuning measurements during 2017 commissioning at $\beta^* = 0.3\,\mathrm{m}$/flat-orbit demonstrated an excellent correction of the IR-b_4, observations at $\beta^* = 0.4\,\mathrm{m}$ with the operational crossing-scheme applied showed a non-negligible increase, potentially indicating feed-down from higher-order errors in the experimental IRs. Measurements of amplitude detuning with and without IR5 crossing-angles applied were performed in 2016 and did not show significant change between the configurations [3, 12]. This implies decapole and dodecapole errors in IR5 are small at present. No comparable study had been performed in IR1 however, and given the potential implications to beam stability during operation with crossing angles it was decided to check the influence of IR1 vertical crossing-angle on amplitude detuning.

Figure 5 shows tune shift versus horizontal action measured for two signs of the IP1 vertical crossing angle. Kicks were only performed in the horizontal plane due to aperture constraints with

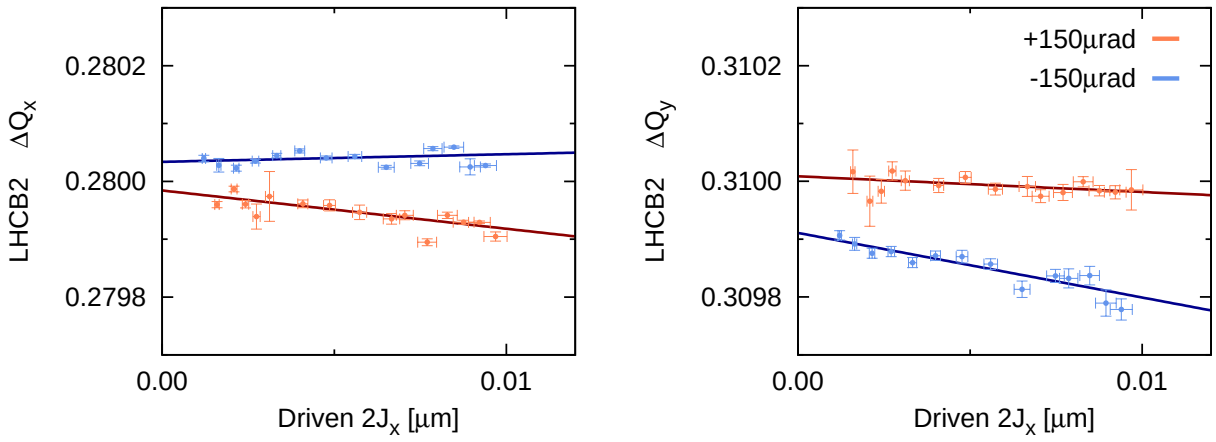

Figure 5: Amplitude detuning of Beam 2 in the horizontal plane, for vertical crossing angles in IP1 of $\pm 150\,\mu\mathrm{rad}$.

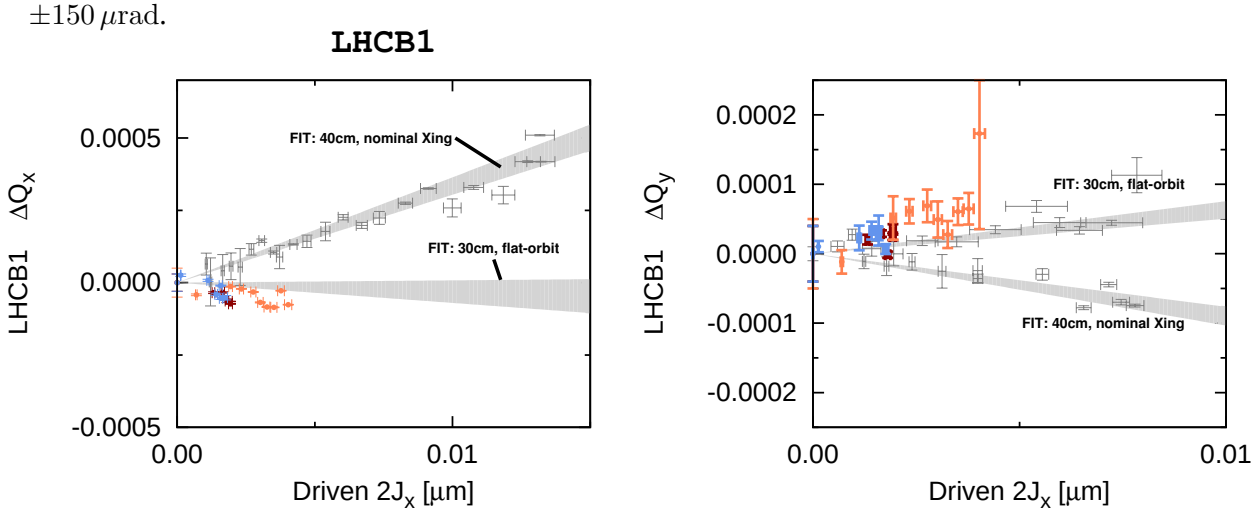

Figure 6: Amplitude detuning of Beam 1 in the horizontal plane, for vertical crossing angles in IP1 of $\pm 150\,\mu\mathrm{rad}$.

large vertical orbit excursions in the IR. The measured kick data has been corrected for drifts of the unperturbed tune as measured by the LHC BBQ. Very small detuning was measured in both cases. It is possible that some marginal change to the detuning was observed between the two crossing angles, however these shifts are negligible compared to detuning generated by either the uncompensated IR-b_4 or the Landau octupoles, and are therefore not relevant to Landau damping during operation.

In Beam 1 an insufficient amplitude range could be probed to provide accurate measurements of the amplitude detuning. Results of the measurements are shown in Fig. 6. Crudely speaking, the data appear consistent with measurements performed at flat-orbit/30cm during 2017 commissioning (shown in gray), and does not explain the anomalous observation at $40\,\mathrm{cm}$ during 2017 commissioning.

Table 3 gives values for the first order detuning coefficients of Beam 2 obtained from the AC-dipole measurements (with direct terms adjusted for the impact of the driven oscillation). Values obtained from measurements at flat-orbit and with the full operational crossing-scheme during 2017 commissioning are also provided. Between $\pm 150\,\mu\mathrm{rad}$ of the IP1 vertical crossing-angle, shifts to the detuning of the order of $4\times10^3\,\mathrm{m}^{-1}$ and $8\times10^3\,\mathrm{m}^{-1}$ were observed for the direct- and cross-terms respectively. This does not explain earlier observations of the detuning at $0.4\,\mathrm{m}$ with the complete

crossing-scheme, which were substantially larger. This motivates additional studies with the complete crossing-scheme and improved control of unperturbed tune drift at flattop and end-of-squeeze to identify sources in IR2/8.

Table 3: Measured first-order detuning coefficients obtained from linear fits to AC-dipole detuning data. Quoted coefficients have been adjusted for the effect of the driven oscillations. Quoted uncertainties are the $1\,\sigma$ standard error on the fit parameters. The reduced χ^2 is given as a measure of goodness of fit. Fits are performed via orthogonal distance regression (ODR).

	$\partial Q/\partial(2J)$ $[10^3\mathrm{m}^{-1}]$				
	Simulation: ($I_{\mathrm{MO}} = 340$ A)	2017 commissioning: (0.3 m, flat-orbit)	2017 commissioning: (0.4 m, crossing-scheme)	MD: IR1@150 μrad	MD: IR1@-150 μrad
$\frac{\partial Q_x}{\partial(2J_x)}_{\mathrm{LHCB2}}$	$+89.5$	-2 ± 1	-3 ± 1	-3 ± 1 ($\chi^2_{red} = 5.5$)	0.7 ± 0.7 ($\chi^2_{red} = 14.8$)
$\frac{\partial Q_y}{\partial(2J_x)}_{\mathrm{LHCB2}}$	-68.4	-3 ± 1	23 ± 4	-3 ± 1 ($\chi^2_{red} = 0.7$)	-11 ± 1 ($\chi^2_{red} = 1.4$)

3.3 Optics measurements with strong skew sextupoles

Figure 7 shows a histogram of the absolute value of f'_{0030} (an AC-dipole RDT closely related to the strength of the $3Q_y$ resonance [6]), as measured in all available BPMs around the ring. Red data indicates the RDT measured with beam-based corrections applied for the a_3 errors in IR1 (found during 2017 commissioning). The correction which reduced the RDT to the level shown in Fig. 7 (red) corresponds to approximately a $20\,\mathrm{A}$ powering of the MCSSX in IR1. Blue data shows the RDT measured when the a_3 corrector on the right side of IP1 (MCSSX3.R1) was powered to its maximum current of $+100\,\mathrm{A}$. With the a_3 artifically increased in this manner the LHC is placed in a state which (very crudely) resembles that which might be expected in the HL-LHC with uncompensated a_3 errors. In the enhanced configuration, it was possible to measure spectral lines corresponding to a_3 sources even at AC-dipole excitation amplitudes typically used for linear optics studies. Normally measurement of the RDTs requires a dedicated, and comparatively slow, ramp of the excitation amplitude. In the HL-LHC, uncompensated sextupole errors in the IRs should be parasitically observable during linear optics measurements. Further analysis should be performed to compare the change in RDTs with predictions from simulation.

Of particular interest in respect to the RDT measurements, is that for the $\pm 150\,\mu\mathrm{rad}$ crossing-angles in IP1, clear shifts to the a_3 RDTs could be observed, most probably resulting from feed-down of b_4. As measurements were performed with the beam-based b_4 corrections applied (which had successfully compensated amplitude detuning globally, and gave significant reductions to second-order feed-down of $b_4 \rightarrow b_2$) it will be important to understand whether the observed shifts in f'_{0030} point to a non-locality of the b_4 correction, or whether this represents the minimimal residual for b_4 feed-down which can be obtained while optimizing normal octupole corrections on the amplitude detuning. In either case this observation clearly demonstrates the potential of feed-down to sextupole RDTs as a new observable for compensation of IR-nonlinear errors. It also highlights the relative significance of the sextupole and octupole errors, since the residual variation of f'_{0030} due to feed-down is comparable to that naturally generated by skew sextupole sources. Given such a situation, the difficulty in finding appropriate corrections for sextupole errors (as exhibited in Sec. 3.1) is hardly surprising.

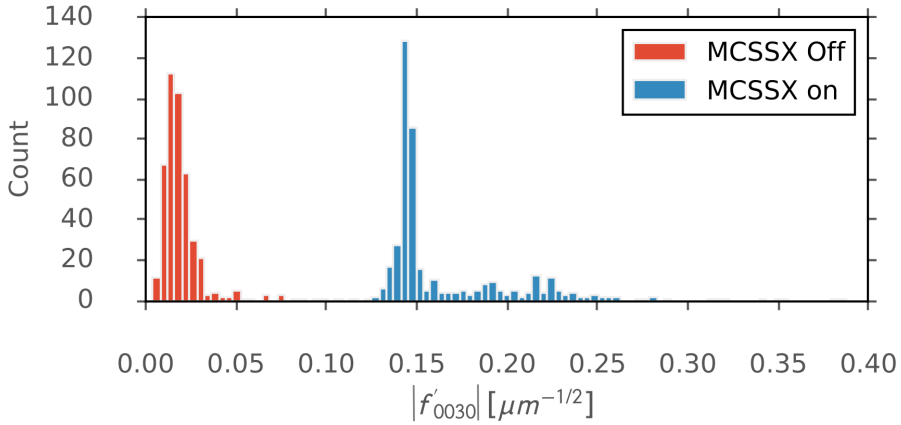

Figure 7: Histogram of $|f'_{0030}|$ over all LHC BPMs, with beam-based corrections for a_3 errors applied (red), and with the MCSSX3.R1 used to artificially bolster a_3 sources to a state representative of low-β operation of the HL-LHC.

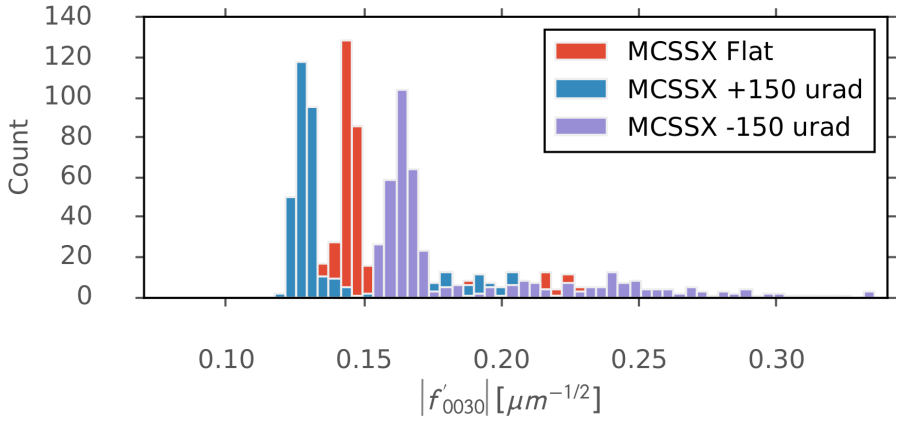

Figure 8: Histogram of $|f'_{0030}|$ measured over all LHC BPMs, with strong MCSSX3.R1. Data is shown for flat-orbit and $\pm 150\,\mu\mathrm{rad}$ vertical crossing angles in IR1.

Feed-down from the sextupole errors themselves is also a matter of serious concern. With the vertical crossing-angle in IP1, skew sextupole errors feed-down to generate tune shifts and β-beating (b_3 errors in conjunction with the horizontal crossing angle in IR5 play a similar role). In the HL-LHC these effects may be critical to operation (of comparable or perhaps greater importance than the influence of a_3 on DA) [13, 14]. During 2017 commissioning feed-down from a_3 errors in IR1 was compensated by powering the MCSSX to minimize linear variation of the tune shift with crossing-angle. This was also observed to significantly improve the strength of the $3Q_y$ resonance, and the differential β-beat between $\pm 150\,\mu\mathrm{rad}$. Global correction for β-beat was then implemented to optimize the linear optics at the operational crossing-scheme.

As β^* is reduced the impact of feed-down will increase. At end-of-squeeze in the HL-LHC, the quadrupole perturbation from feed-down of uncompensated nonlinear errors in the IR, can become comparable to that generated by the linear LHC triplet errors at $\beta^* = 1\,\mathrm{m}$. In such a situation it will make sense to adapt the nonlinear commissioning strategy to make use of observables and correction methods tailored to the compensation of large local errors in the IRs. Specifically the *Segment-by-Segment* (SbS) technique [9, 10], which has been used in the commissioning of the linear optics of the IRs since the LHC first began operation. This is of interest both as a new observable to determine

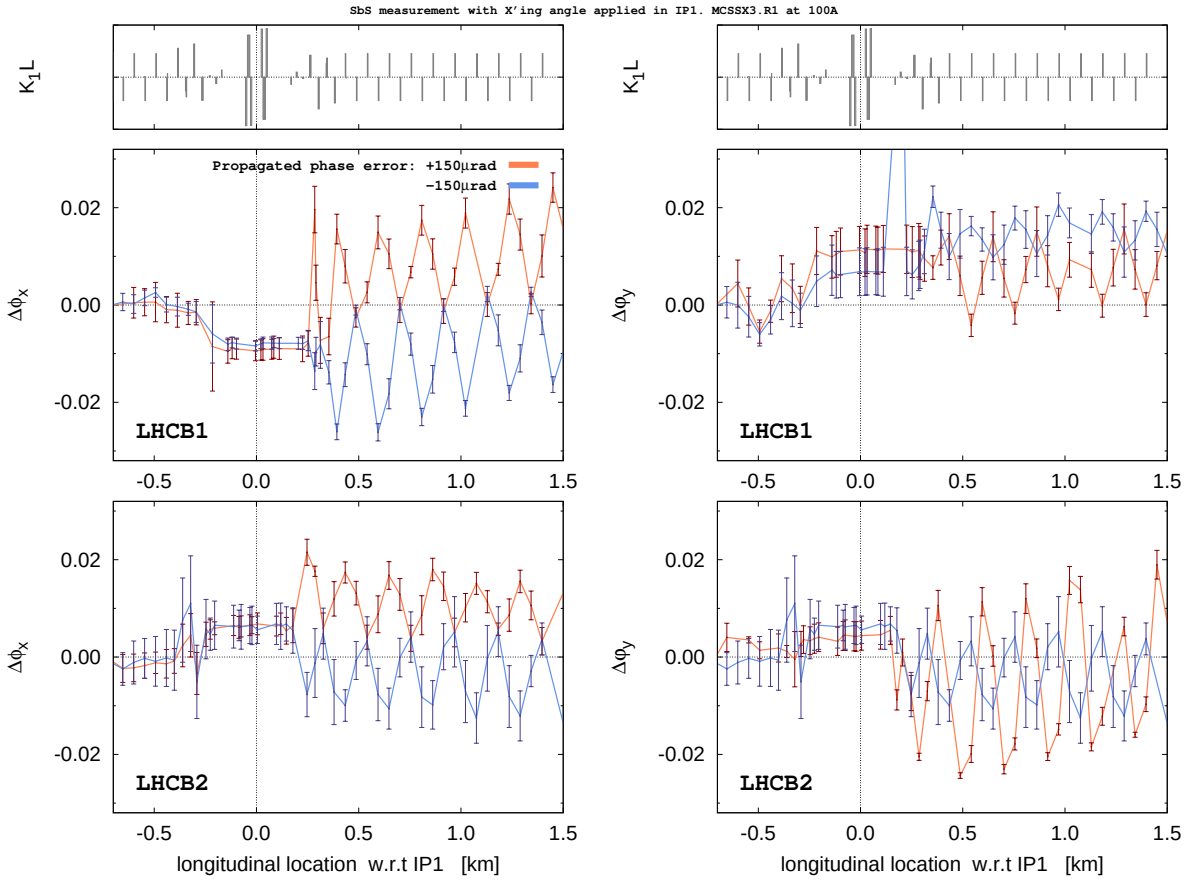

Figure 9: Propagated phase error through IR1 obtained with the segment-by-segment method. Data is shown for Beam 1 (left) and Beam 2 (right), for positive and negative signs of the vertical crossing-angle in IP1.

corrections with the MCSSX, and to apply local corrections for the residuals using insertion quads (superseding the global optimization utilized so far). As a first step in this direction it was desired to attempt to measure the local phase advance error through IP1 with the segment-by-segment method, with two signs of the vertical crossing-angle in the enhanced-a_3 configuration previously described. Compared to the LHC at $\beta^* = 0.4\,\mathrm{m}$, it is crudely expected that the feed-down from a comparable nonlinear error should be appriximately a factor 5 larger at end-of-squeeze in HL-LHC (a factor ~ 2.5 from linear scaling of the feed-down to quadrupole with β^{*-1} and a factor ~ 2 from the larger crossing angles in HL-LHC). The $100\,\mathrm{A}$ powering of the MCSSX is therefore a representative (although very crude) scaling of the feed-down from the uncompensated IR1 a_3 errors (compensated by $20\,\mathrm{A}$) to HL-LHC-like conditions. The deviation of the propagated phase advance with respect to the nominal model, obtained via the SbS technique for $\pm 150\,\mu\mathrm{rad}$ in IP1 is shown in Fig. 9.

The effect of the large skew sextupole source can be clearly seen, while the propagated phase error is indeed comparable to cases where local compensation of the linear triplet errors has been successfully applied in Run 1. Direct local, as opposed to global, compensation of the quarupole errors generated by sextupole feed-down should be viable in the HL-LHC. The SbS method has also proved effective in localizing linear errors within the LHC IRs. Having performed a first test of the SbS method as a means to examine the sextupole sources, it will also be of interest to follow up in simulation whether the SbS can prove more effective than simple tune measurements as a means to identify and localize sextupole sources within the IRs.

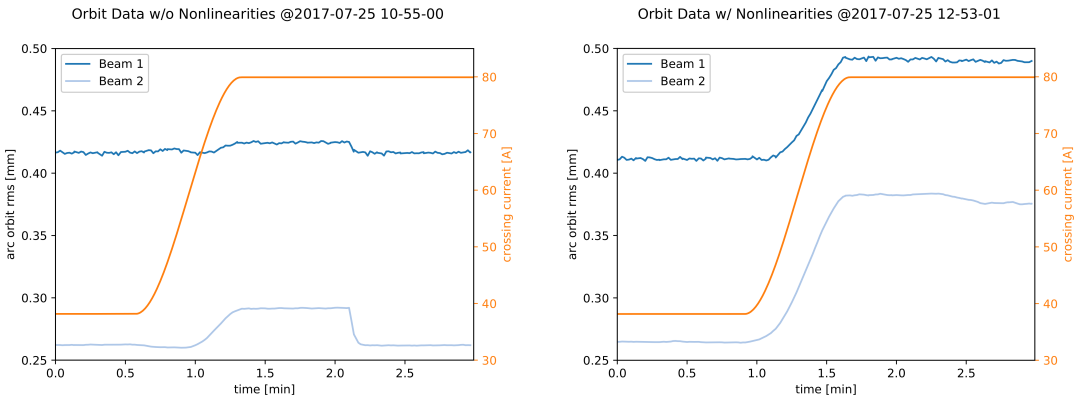

Figure 10: RMS arc orbit measured during application of the IP1 vertical crossing-angle, with beam-based a_3 corrections applied (left) and with a_3 artificially increased using the MCSSX3.R1 (right).

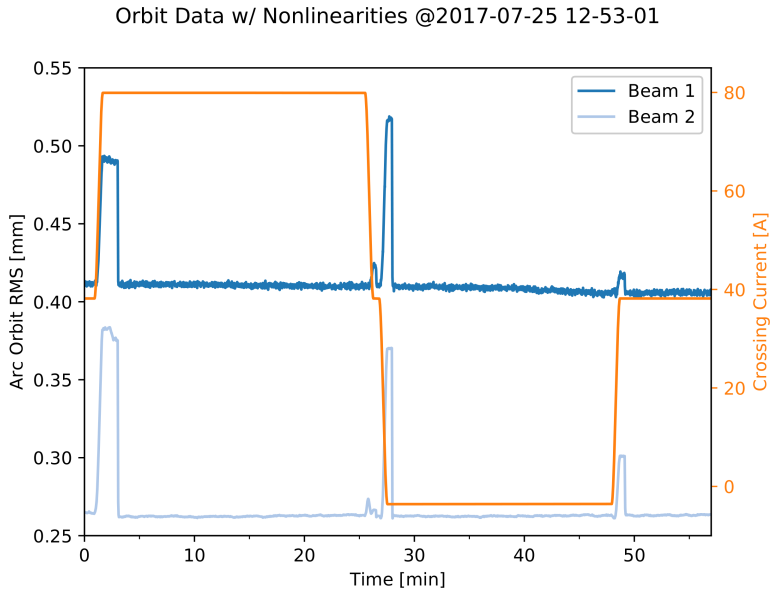

Figure 11: RMS arc orbit measured for various changes in the IP1 vertical crossing-angle. Leakage corrections with the orbit feed-back have been applied.

As the sextupole errors become more significant, the possibilities to measure are clearly improved. However such large nonlinearities also introduce new challenges to operation. It was observed when applying the crossing-angles with strong MCSSX3.R1, that leakage from the IR1 crossing-angle bump was considerably worse than with well corrected a_3 sources. Figure 10 (left) shows the RMS closed orbit measured in the LHC arcs as the IP1 vertical crossing-angle is trimmed to $+150, \mu\mathrm{rad}$ with the beam-based a_3 corrections applied. Figure 10 (right) shows the same measurement and procedure, but with a_3 errors enhanced by the strong powering of MCSSX3.R1.

Orbit leakage during crossing-angle scans is of considerable concern to commissioning of the nonlinear optics, since leakage to the IPs not under investigation can compromise the measurments. Fortunately the leakage observed in Fig. 10 could be well controlled with the orbit feed-back (OFB), as seen in Fig. 11. While not of critical concern therefore, this behaviour will have to be monitored during any optics commissioning of the LHC or HL-LHC with strong nonlinearities in the IRs.

Figure 12 compares the nominal $+150\,\mu\mathrm{rad}$ crossing-angle bump from MAD-X to that measured in LHC BPMs before (gray) and after (colour) application of the OFB. While an effect on

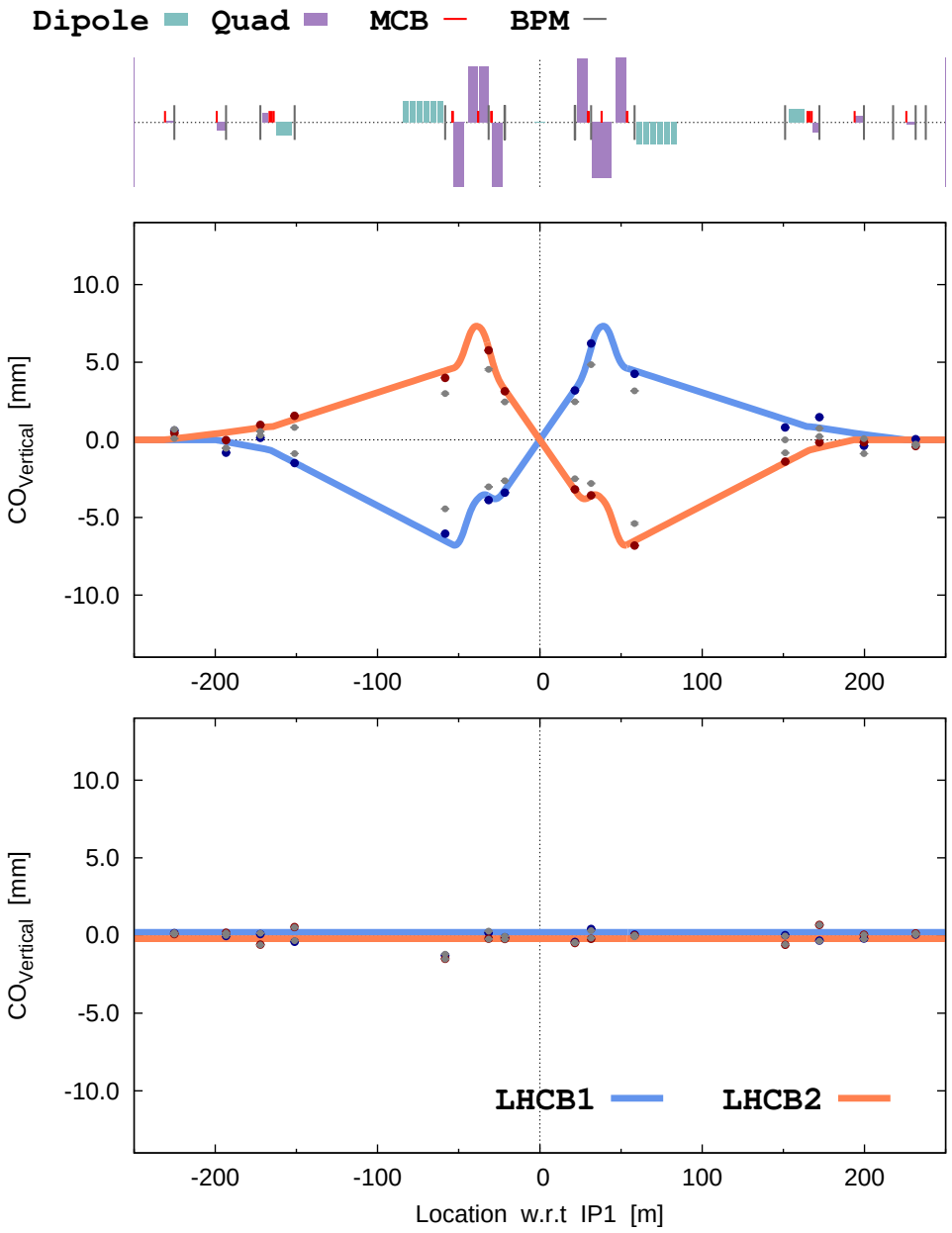

Figure 12: Modelled and measured orbit in the IR1.

the crossing angle can be seen before the OFB was applied, after application the measured bump shows an excellent agreement with the expected closed orbit, with the same degree of accuracy as obtained with well corrected a_3. While sextupole feed-down can have a non-negligible influence on the closed-orbit, both in regard to crossing angle and leakage, this appears straightforaward to control during measurements with the relevant feed-back.

Of far more profound concern to the optics measurement and correction prospects of the HL-LHC was an observation that AC-dipole excitation in the enhanced a_3 configuration led to a dramatic blow-up of the LHC beams. Figure 13 shows the $1\,\sigma$ beam-size of Beam 1, as recorded by the BSRT both before and after the a_3 errors were enhanced with the MCSSX. With beam-based corrections for a_3 applied, no blow-up was observed during linear optics measurements, and only slight increase in beam-size was observed during amplitude detuning measurements. In contrast, after the a_3 was enhanced even the very small kicks used to perform segment-by-segment measurements (which at

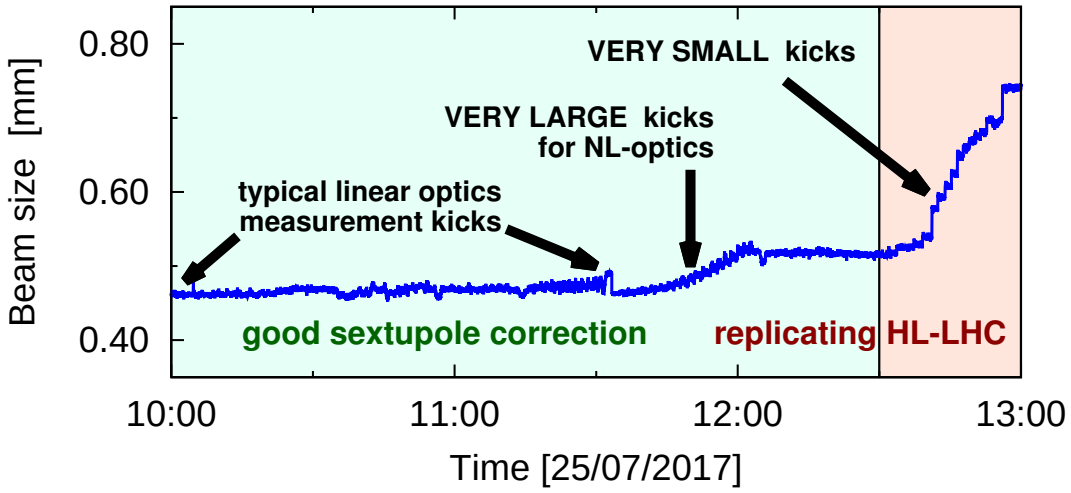

Figure 13: Beam size of LHCB1 during AC-dipole exciting with and without enhancement of the skew sextupole sources with MCSSX.

$1.3\,\mathrm{mm}$ peak-to-peak were already small compared to the typical $2\,\mathrm{mm}$ kicks used for linear optics commissioning) resulted in dramatic blow-up.

The mechanism leading to increase of beam-size during AC-dipole excitation is unclear. To first order the nonlinear RDTs are not expected to lead directly to loss of adiabaticity during the AC-dipole ramp [6], though it is unclear the extent to which the width of the $3Q_y$ stop-band, and detuning, chromaticity and chromatic coupling generated by the a_3 source may compromise this assumption. Alternatively the blow-up may reflect a reduction of dynamic aperture for the duration driven oscillations are applied [15], leading to diffusive beam-growth during AC-dipole excitation, followed by particles then becoming frozen in newly stable orbits upon the end of excitation. Given the small kick amplitudes considered however, this would represent a dramatic degradation of dynamic aperture in the presence of forced oscillations. Either case, direct loss of AC-dipole adiabaticity or indirect loss of adiabaticity due to chaotic diffusion during excitation, represents an interesting topic for study which should be followed up in simulation.

Regardless of the underlying mechanism however, loss of AC-dipole adiabaticity (as seen in Fig. 13) presents a very serious challenge to HL-LHC commissioning. After around 12 kicks with the strong-a_3 configuration Beam 1 was rendered to all intents and purposes unusable for the remainer of the MD. To place this figure in context it should be considered that the low-β^* commissioning of the LHC in 2017 required $\sim 460\,\mathrm{kicks}$ at $\beta^* \leq 0.6\,\mathrm{m}$. Commissioning strategy can be adapted: for example through greater emphasis corrections calculated from magnetic and alignment data, or through an itterative approach to linear and nonlinear commissioning at progressively smaller β^*. However, it will still be essential to follow up this observation with further studies in the LHC to understand the implications uncompensated nonlinearities and failing nonlinear correctors have upon our ability to measure and correct even the linear optics at low-β^* in the HL-LHC, in addition to understanding whether other higher-order errors can generate similar behaviour. One possible strategy for mitigation would be to attempt to find a more optimal working point for the natural and driven oscillations, however this too will require further study in the machine.

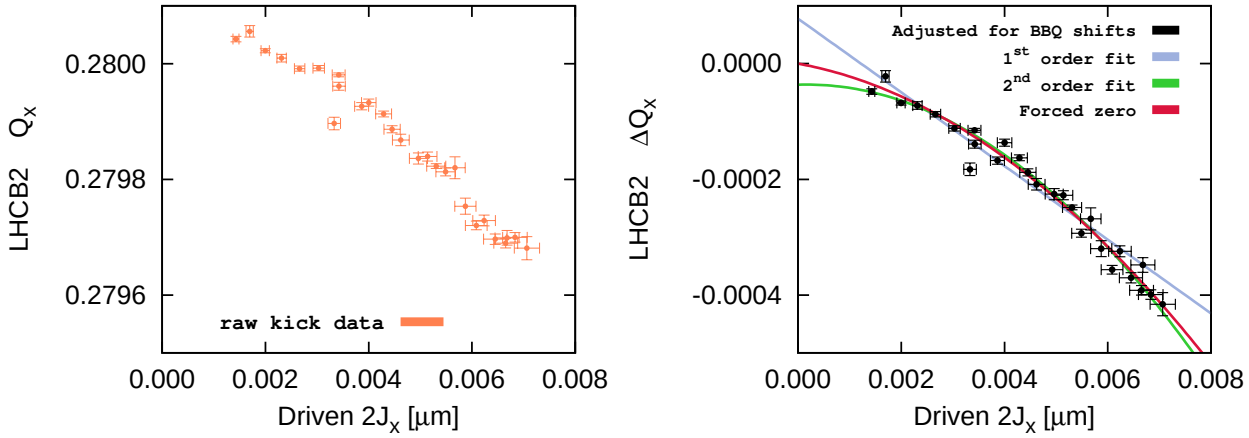

Figure 14: Measured change of Q_x with horizontal amplitude in LHC Beam 2, for uniform $50\,\mathrm{A}$ powering of the MCTX in IR1 and 5. Measurements were performed at flat-orbit

3.4 Optics measurements with strong dodecapoles

Dodecapole correction in the HL-LHC experimental insertions is of considerable concern, with a significant impact of these errors expected on dynamic aperture. No dodecapole compensation has been attempted so far in the LHC, where the errors have not yet appeared to become operationally relevant. Correction of b_6 is expected to be particularly challenging largely due to the relative paucity of well established observables from which to determine beam-based corrections. Direct compensation of lifetime or dynamic aperture is one possibility, however DA measurement lacks the straighforward relationship to b_6 which would facilitate precise correction, and with four correctors and a single observable would necessarily represent an underconstrained problem. Experience of LHC commissioning has also well established the benefits arising from compensation and validation based on a combination of observables.

Amplitude detuning potentially represents a complementary observable to dynamic aperture for b_6. A global measure of the b_6, weighted according to the β-functions at the location of the errors, can be obtained by examining second-order detuning with amplitude detuning at flat-orbit. A local observable to each IR can be obtained by considering the feed-down from $b_6 \rightarrow b_4$, generating a change of the first-order detuning terms as a function of crossing-angle. As a first test of these observables dodecapole sources in the IRs were artifically enhanced by powering all MCTX in IR1 and IR5 to $50\,\mathrm{A}$ ($K_6 = 24950.0\,\mathrm{m}^{-6}$). Amplitude detuning was measured with the AC-dipole following the usual procedure. It was only possible to perform the measurement on LHC Beam 2 due to earlier blow-up of Beam 1 preventing a sufficient amplitude range being probed. For this first test measurements were only performed in the horizontal plane. The natural tune was not visible in the vertical spectrum, likely due to intensity loss earlier in the MD resulting in a degraded BPM signal when measuring with smaller beam currents towards the end of the session. The variation of horizontal tune with horizontal amplitude could however, be observed over a sufficient amplitude range to study the detuning. The raw variation of tune with amplitude obtained from the AC-dipole kicks is shown in Fig. 14 (left).

Some variation of the unperturbed tune could be seen in BBQ data during the amplitude detuning study, however noise on the measurement was large. Figure 15 shows a moving average window applied to the BBQ data. This moving average was used as a reference for the tunes obtained from the AC-dipole kicks. Adjusted data is shown in Fig. 14 (right). The impact of the tune variation on measured detuning was small.

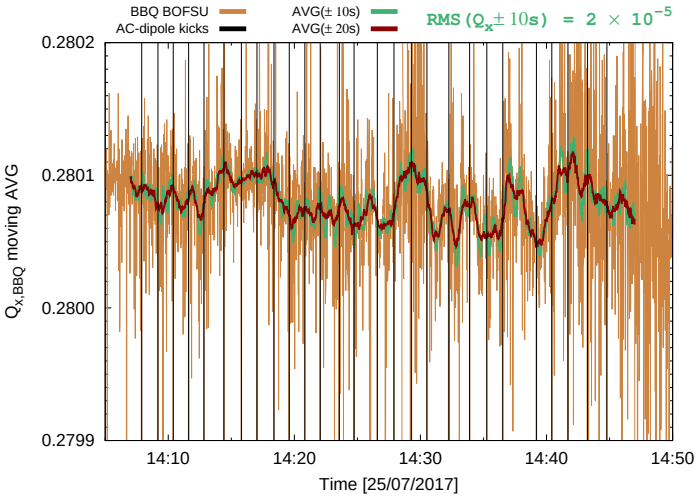

Figure 15: Horizontal tune of LHC Beam 2 monitored by the BBQ throughout amplitude detuning measurements with strong MCTX.

Table 4 shows the results of fits of detuning coefficients to the BBQ adjusted data (controlling for the influence of driven oscillation). Only including the first-order coefficient gives a low quality of fit as characterized by the χ^2_{red} statistic. The exact value of the second-order coefficient is somewhat sensitive to whether or not the unperturbed tune at $J_x = 0$ is forced to the value obtained from the LHC BBQ. If left as a free parameter, the unperturbed tune shows a deviation from the value given by the BBQ of around 4×10^{-5}. This can result from a tune offset due to the small vertical kick (due to cross-term detuning) which is held constant during the horizontal detuning measurement, however as the cross-terms do not feature any enhancement from driven oscillations, and the quadratic shift should not generate significant tune shifts at small amplitudes this seems unlikely. If the fits of detuning coefficients are forced to value of the BBQ at zero amplitude the second order term changes by around $25\,\%$. To improve this situation would require more tune data at smaller amplitudes. It may be possible to achieve improved resolution in future measurements if intensity can be better preserved throughout the nonlinear studies. The measured second-order detuning agrees within the standard fit error, to the value predicted by PTC for this setting of the MCTX.

Following measurement at flat-orbit it was attempted to measure detuning with the vertical crossing angle of IP1 set to $+150\,\mu\mathrm{rad}$. Due to high losses this measurement was abandoned, and the crossing angle was instead trimmed to $+75\,\mu\mathrm{rad}$. Figure 16 show the unperturbed tune recorded by the BBQ during the amplitude detuning measurement. This data was used to compensate AC-dipole kicks for changes to the unperturbed tune. Figure 17 shows the raw AC-dipole data (left) and corrected data (right) together with fits of the detuning coefficients. The detuning clearly changed upon application of the crossing-angle.

Table 5 compares detuning coefficients obtained through various fits to the measured data. While a clear change to the detuning can be observed in Fig. 17, the comparatively small number of data points and small amplitude range limits the ability to draw quantitative conclusions from the measurement, particularly due to corellations between the first and second order terms in the polynomial fit. As such the change of first order detuning with crossing-angle looks at present to be a useful method for validation of local b_6 correction, but of limited use to actually calculate the correction in the first instance. Further studies will be required to see if this limitation can be surpassed, in par-

Table 4: Detuning coefficients obtained from fits to adjusted AC-dipole tune shift data, for several different fitted functions. Factors $\mathbf{2}\times$ and $\mathbf{3}\times$ in the detuning equations correspond to the enhancement of direct detuning terms by a factor $n/2$ (where $n = 4$ implies octupole, $n = 6$ implies dodecapole...) due to the driven oscillations. The second order detuning coefficient obtained from PTC_NORMAL for the applied powering of MCTX is also shown. These results correspond to measurement at flat-orbit, with a uniform 50 A powering of MCTX in IR1 and IR5.

χ^2_{red}	ΔQ_{x0}	$\partial Q_x/\partial(2J_x)$ $[10^3\mathrm{m}^{-1}]$	$\partial^2 Q_x/\partial(2J_x)^2$ $[10^{12}\mathrm{m}^{-2}]$
FIT: $\Delta Q_0 + \left(2 \times \frac{\partial Q}{\partial(2J)}\right)$			
16.1	0.00008 ± 0.00001	-32 ± 2	-
FIT: $\Delta Q_0 + \left(2 \times \frac{\partial Q}{\partial(2J)}\right) + \left(3 \times \frac{1}{2!}\frac{\partial^2 Q}{\partial(2J)^2}\right)$			
5.8	-0.00004 ± 0.00002	1 ± 5	-5.5 ± 1
FIT: $0.0 + \left(2 \times \frac{\partial Q}{\partial(2J)}\right) + \left(3 \times \frac{1}{2!}\frac{\partial^2 Q}{\partial(2J)^2}\right)$			
6.3	-	-8 ± 1	-4.1 ± 0.4
Simulation with uniform $K_{\mathrm{MCTX}} = 24950.0\,\mathrm{m}^{-6}$ in IR1/5			
-	0.0	1	-4.5

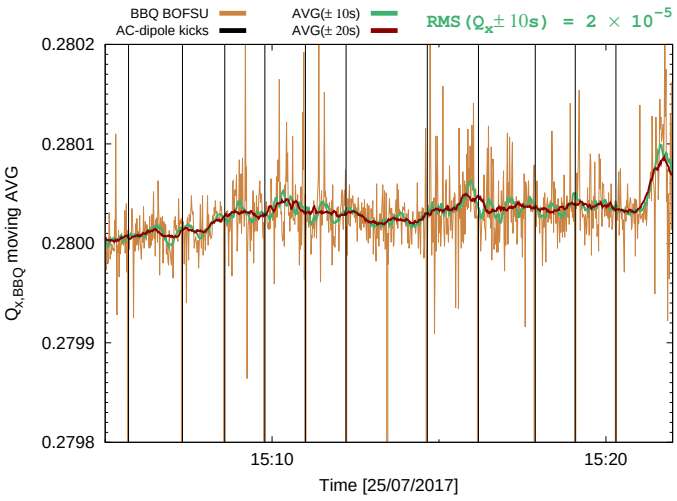

Figure 16: Horizontal tune of LHC Beam 2 monitored by the BBQ throughout amplitude detuning measurements with strong MCTX and $+75\,\mu\mathrm{rad}$ crossing-angle.

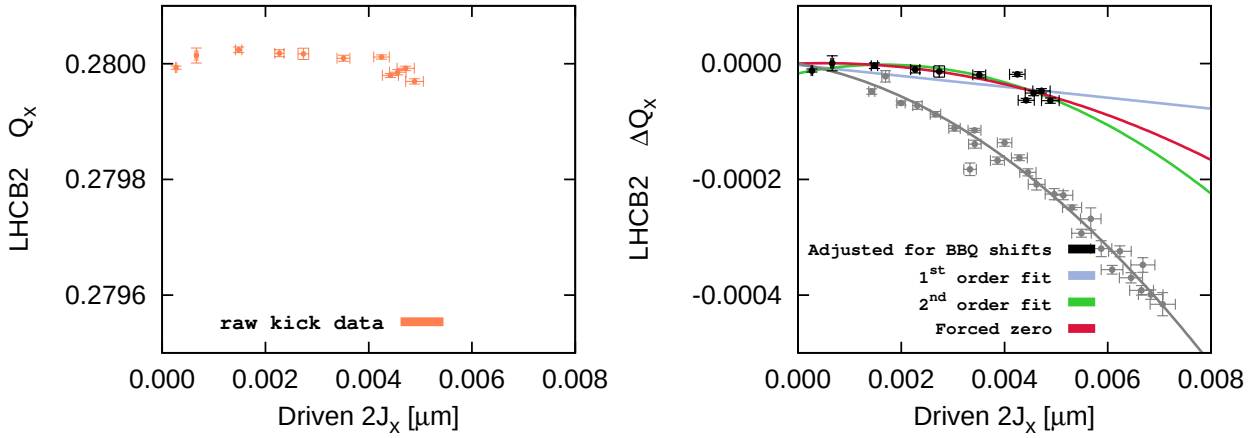

Figure 17: Measured change of Q_x with horizontal amplitude in LHC Beam 2, for uniform $50\,\mathrm{A}$ powering of the MCTX in IR1 and 5, and $+75\,\mu\mathrm{rad}$ crossing-angle in IR1. Grey data indicates the measurement performed with strong MCTX at flat orbit (shown previously in Fig. 14).

ticular whether measurement with better beam-current and over a larger amplitude range can help remove corellation between the first and second order terms.

Table 5: Detuning coefficients obtained from fits to adjusted AC-dipole tune shift data, for several different fitted functions. Factors $\mathbf{2}\times$ and $\mathbf{3}\times$ in the detuning equations correspond to the enhancement of direct detuning terms by a factor $n/2$ (where $n = 4$ implies octupole, $n = 6$ implies dodecapole...) due to the driven oscillations. The second order detuning coefficient obtained from PTC_NORMAL for the applied powering of MCTX is also shown. These results correspond to measurement with a uniform $50\,\mathrm{A}$ powering of MCTX in IR1 and IR5, and a $+75\,\mu\mathrm{rad}$ crossing angle in IR1.

χ^2_{red}	ΔQ_{x0}	$\partial Q_x/\partial(2J_x)$ $[10^3\mathrm{m}^{-1}]$	$\partial^2 Q_x/\partial(2J_x)^2$ $[10^{12}\mathrm{m}^{-2}]$
FIT: $\Delta Q_0 + \left(2\times\frac{\partial Q}{\partial(2J)}\right)$			
13.0	0.00000 ± 0.00001	-5 ± 1	-
FIT: $\Delta Q_0 + \left(2\times\frac{\partial Q}{\partial(2J)}\right) + \left(3\times\frac{1}{2!}\frac{\partial^2 Q}{\partial(2J)^2}\right)$			
8.4	-0.00002 ± 0.00001	9 ± 5	-3.7 ± 2
FIT: $0.0 + \left(2\times\frac{\partial Q}{\partial(2J)}\right) + \left(3\times\frac{1}{2!}\frac{\partial^2 Q}{\partial(2J)^2}\right)$			
10.4	-	$+2 \pm 4$	-2 ± 1

As previously mentioned, attempts to measure detuning at $+150\,\mu\mathrm{rad}$ failed due to increased losses with kicks following application of the crossing angle. A peak-to-peak amplitude of $1\,\mathrm{mm}$ could not be exceeded. In contrast, the flat-orbit measurement with strong MCTX performed immediately prior was able to reach $\sim 2.4\,\mathrm{mm}$ peak-to-peak with little difficulty. Figure 18 shows beam losses recored by the Beam 1 (red) and Beam 2 (blue) BLMs located at the primary collimators. The green area of plot represents kicks performed at $+150\,\mu\mathrm{rad}$. Losses at flat-orbit, even with strongly powered MCTX, are characteristic of typical AC-dipole excitation: a sharp spike in

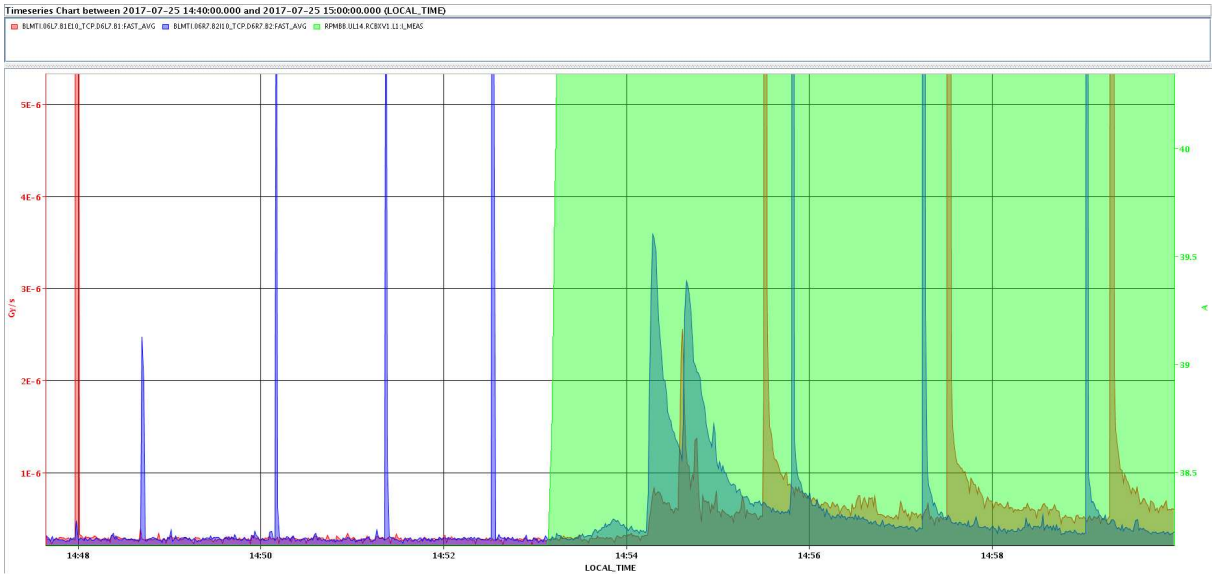

Figure 18: BLM data for AC-dipole kicks performed before (white region) and after (green region) application of the IR1 crossing-angle with strong MCTX.

the BLM signal followed by a return to the previous level of losses. In contrast, kicks performed with the crossing-angle applied show persistent losses which slowly decay following the kick. This is characterisic of beam-loss on the single-particle dynamic aperture. Figure 14 provides a strong indication that feed-down from dodecapole errors may be of greater importance to dynamic aperture than the direct impact of the b_6 itself. Clearly this has only been seen in a single configuration so far, however since optimized settings of the MCTX can change depending on whether feed-down or direct-b_6 is the preferred target of correction, these observations should be followed up to help define the commissioning strategy for HL-LHC.

4 Conclusions

MD 2158 was very successful. All desired measurements were completed in some form. Four new observables for IR-nonlinear errors were tested for the first time: RDT variation with crossing angle, application of the segment-by-segment method to sextupole feed-down, second-order detuning for b_6, and feed-down from b_6 to change first-order detuning versus crossing angle. The first observation of second-order amplitude detuning, in good agreement with the expectation from theory/simulation, is particularly encouraging in view of HL-LHC commissioning. Useful information was gained in regard to the $a_{3,4}$ errors in IR5, which has helped plan 2018 commissioning strategy. New topics for study in regard to commissioning strategy for the HL-LHC have also been revealed, in particular comparing the relative importance to dynamic aperture of b_6 feed-down as opposed to the b_6 errors themselves, as well as the potentially very serious question of loss of AC-dipoole adiabaticity in the presence of strong nonlinear errors.

5 Acknowledgments

Many thanks go to the OP and BI groups for the support lent to these studies. Similarly thanks go to the collimation team for helping facilitate the large amplitude kicks necessary for nonlinear measurements in the LHC.

References

[1] E.H. Maclean. "New optics correction approaches in 2017". Presentation to the 8th Evian Workshop (Evian, 12 December 2017) (2017).
https://indico.cern.ch/event/663598/contributions/2781846/attachments/1573573/2483868/2017_12_Evian.pdf

[2] E.H. Maclean. "New optics correction approaches in 2017". Proceedings of the 8th Evian Workshop (Evian, 12 December 2017) (2017).

[3] M.S Camillocci K. Fuchsberger M. Giovannozzi T.H.B. Persson R. Tomás E.H. Maclean, F. Carlier. "Report from LHC MDs 1391 and 1483: Tests of new methods for study of nonlinear errors in the LHC experimental insertions" (2017).

[4] E.H. Maclean, T.H.B. Persson and R. Tomás. "Amplitude dependent closest tune approach generated by normal and skew octupoles". In "Proc. IPAC'17, Copenhagen, Denmark.", Number WEPIK091 (2017).
http://accelconf.web.cern.ch/AccelConf/ipac2017/papers/wepik091.pdf

[5] E.H. Maclean. "IR-nonlinear errors: 2017 experience & implications for HL-LHC". Presentation to the HL-LHC WP2 working group (CERN, 19 December 2017) (2017).
https://indico.cern.ch/event/685264/contributions/2824696/attachments/1577454/2491426/2017-12-19_wp2.pdf

[6] R. Tomás. "Normal form of particle motion under the influence of an ac dipole", Phys. Rev. ST. Accel. Beams, **5**, 054001.
https://journals.aps.org/prab/abstract/10.1103/PhysRevSTAB.5.054001

[7] E.H. Maclean. "IR-nonlinear commissioning in 2017". Presentation at the CERN ABP-HSS section meeting, 31st May 2017 (2017).
https://indico.cern.ch/event/640288/

[8] E.H. Maclean. "First commissioning of nonlinear errors in experimental insertions". Presentation at the CERN LHC Machine Committee, 19th July 2017 (2017).
https://indico.cern.ch/event/654265/

[9] M. Aiba, S. Fartoukh, A. Franchi, M. Giovannozzi, V. Kain, M. Lamont, R. Tomás, G. Vanbavinckhove, J. Wenninger, F. Zimmermann, R. Calaga and A. Morita. "First β-beating measurement and optics analysis for the CERN Large Hadron Collider", Phys. Rev. ST. Accel. Beams, **12**, 081002.
http://prst-ab.aps.org/abstract/PRSTAB/v12/i8/e081002

[10] R. Tomás, O. Bruning, M. Giovannozzi, P. Hagen, M. Lamont, F. Schmidt, G. Vanbavinckhove, M. Aiba, R. Calaga and R. Miyamoto. "CERN Large Hadron Collider optics model, measurements, and corrections", Phys. Rev. ST. Accel. Beams, **13**, 121004.
http://prst-ab.aps.org/abstract/PRSTAB/v13/i12/e121004

[11] E.H. Maclean, F. Carlier, M. Giovannozzi, T.H.B. Persson and R. Tomás. "Effect of linear coupling on nonlinear observables at the LHC". In "Proc. IPAC'17, Copenhagen, Denmark.", Number WEPIK092 (2017).
http://accelconf.web.cern.ch/AccelConf/ipac2017/papers/wepik092.pdf

[12] E.H. Maclean, F.S. Carlier, J.M. Coello de Portugal, A. Garcia-Tabares, M. Giovannozzi, L. Malina, T.H.B Persson, P.K. Skowronski and R. Tomás. "New methods for measurement of nonlinear errors in LHC experimental IRs and their application in the HL-LHC". In "Proc. IPAC 17. Copenhagen, Denmark.", Number WEPIK093 (2017).
http://accelconf.web.cern.ch/AccelConf/ipac2017/papers/wepik093.pdf

[13] E.H. Maclean. "Prospect for correction of nonlinear errors in HL-LHC experimental insertions". 6th HL-LHC collaboration Meeting (Paris, 14-16 November 2016) (2016).
https://indico.cern.ch/event/549979/contributions/2263212/attachments/1371461/2081287/2016-11-15_IRNLcorrecitons.pdf

[14] F. Carlier, J. Coello, S. Fartoukh, E. Fol, A. García-Tabares, M. Giovannozzi, M. Hofer, A. Langer, E.H. Maclean, L. Malina, L. Medina, T.H.B. Persson, P. Skowronski, R. Tomás, F. Van der Veken and A. Wegscheider. "Optics Measurement and Correction Challenges for the HL-LHC" (2017). CERN-ACC-2017-0088.
https://cds.cern.ch/record/2290899

[15] F.S. Carlier and R. Tomás. "First Demonstration of Dynamic Aperture Measurements with an AC dipole". Unpublished.